# Disproportionation of Ag(II) to Ag(I) and Ag(III) in Fluoride Systems and Syntheses and Structures of $(AgF^+)_2AgF_4^-MF_6^-$ Salts (M = As, Sb, Pt, Au, Ru)

**Ciping Shen, Boris Žemva,† George M. Lucier, Oliver Graudejus, John A. Allman, and Neil Bartlett***

Chemical Sciences Division, Lawrence Berkeley National Laboratory, and Department of Chemistry, University of California at Berkeley, Berkeley, California 94720

*Received March 10, 1999*

Interaction of $Ag^+$ salts in anhydrous liquid hydrogen fluoride, aHF, with $AgF_4^-$ salts gives amorphous red-brown diamagnetic $Ag^IAg^{III}F_4$, which transforms exothermally to brown, paramagnetic, microcrystalline $Ag^{II}F_2$ below 0 °C. $Ag^IAu^{III}F_4$ prepared from $Ag^+$ and $AuF_4^-$ in aHF has a tetragonal unit cell and a $KBrF_4$ type lattice, with $a = 5.788(1)$ Å, $c = 10.806(2)$ Å, and $Z = 4$. Blue-green $Ag^{II}FAsF_6$ disproportionates in aHF (in the absence of $F^-$ acceptors) to colorless $Ag^IAsF_6$ and a black pseudotrifluoride, $(Ag^{II}F^+)_2Ag^{III}F_4^-AsF_6^-$. The latter and other $(AgF)_2AgF_4MF_6$ salts are also generated by oxidation of $AgF_2$ or $AgF^+$ salts in aHF with $F_2$ or in solutions of $O_2^+MF_6^-$ salts (M = As, Sb, Pt, Au, Ru). Single crystals of $(AgF)_2AgF_4AsF_6$ were grown from an $AgFAsF_6/AsF_5$ solution in aHF standing over $AgF_2$ or $AgFBF_4$, with $F_2$ as the oxidant. They are monoclinic, $P2/c$, at 20 °C, with $a = 5.6045(6)$ Å, $b = 5.2567(6)$ Å, $c = 7.8061(8)$ Å, $\beta = 96.594(9)°$, and $Z = 1$. The structure consists of $(AgF)_n^{n+}$ chains (F−Ag−F = 180°, Ag−F−Ag = 153.9(11)°, Ag−F = 2.003(4) Å), parallel to $c$, that enclose stacks of alternating $AgF_4^-$ and $AsF_6^-$, each anion making bridging contact with four Ag(II) cations of the four surrounding chains "caging" them. There is no registry between the ordered array in one "cage" and that in any neighboring "cage". The F-ligand anion bridges between the anions and, with the Ag(II) of the chains, generates a trifluoride-like structure. $(AgF)_2AgF_4AsF_6$ [like other $(AgF)_n^{n+}$ salts] is a temperature-independent paramagnet except for a Curie "tail" below 50 K.

## Introduction

The Ag(II) oxidation state is peculiar to fluoro-ligand systems. Although, in its ligand-field effects, oxygen is close to fluorine,[1] Ag(II) does not occur in oxides[2,3] where, typically, AgO is $Ag^IAg^{III}O_2$. Attempts to disproportionate $AgF_2$, to prepare $AgF_4^-$, by using highly basic solutions in aHF (in which Ag(I)F and the heavier-alkali-metal $AgF_4^-$ salts are all highly soluble) did not succeed:

$$2AgF_2(c)\ (\text{with } F^- \text{ in aHF}) \not\rightarrow Ag^+(solv) + AgF_4^-(solv) \quad (1)$$

But the stability of $AgF_4^-$ salts toward solvolysis[4] in aHF made it possible to attempt the synthesis of $Ag^IAg^{III}F_4$ in that solvent. The existence[5] of $AgAuF_4$ and the finding here, that this salt has the same structure as its lighter-alkali-metal $AAuF_4$ salts (which are themselves[6] isostructural with their $AAgF_4$ relatives[7]), gave impetus to the notion that $Ag^IAg^{III}F_4$, with such a symmetrical lattice, could, perhaps, have sufficient kinetic stability to be isolable in that form. This hope has not been fully realized (the prepared $Ag^IAg^{III}F_4$ having a particle size too small for structural characterization), but the thermodynamic instability of $Ag^IAg^{III}F_4$ has been confirmed by its exothermic transition to $Ag^{II}F_2$.

Partial disproportionation of Ag(II) to Ag(I) and Ag(III) has, however, been observed in association with the solvolysis of the salt $AgF^+AsF_6^-$ in aHF:

$$4AgFAsF_6(c) \rightarrow AgAsF_6(c) + (AgF)_2AgF_4AsF_6(c) + 2AsF_5(solv) \quad (2)$$

the colorless $AgAsF_6$ (as a consequence of its lower density) sedimenting more slowly than the black product $(Ag^{II}F)_2Ag^{III}F_4AsF_6$ (concisely: $Ag_3AsF_{12}$).

This paper details these findings and provides other synthetic routes to the mixed-valence $Ag_3AsF_{12}$. Syntheses are also given for its isostructural relatives $Ag_3MF_{12}$ (M = Sb, Pt, Au, Ru). Single-crystal X-ray diffraction analysis of $Ag_3AsF_{12}$ has provided a structural basis for all. High thermodynamic stability, deriving from the rather close-packed pseudotrifluoride structure, may be responsible for the ready formation of these Ag(II)Ag(III) mixed-valence compounds.

## Experimental Section

**Apparatus and Techniques.** Work involving aHF was carried out in apparatus constructed entirely from fluorocarbon polymers, T-reactors being made from FEP tubing (CHEMPLAST, Inc., Wayne, NJ 07480) with Teflon valves and Swagelok fittings, as previously described.[8]

† Miller Visiting Professor, UCB (1993), from the Jožef Stefan Institute, University of Ljubljana Jamova 39, 1000 Ljubljana, Slovenia.

(1) Dunitz, J. D.; Orgel, L. E. *Advances in Inorganic Chemistry and Radiochemistry*; Academic Press Inc.; New York, 1960; Vol. 2, pp 1−56.
(2) Jansen, M.; Fischer, P. *J. Less-Common Met.* **1988**, *137*, 123.
(3) Standke, B.; Jansen, M. *Z. Anorg. Allg. Chem.* **1986**, *535*, 39.
(4) Lutar, K.; Jesih, A.; Leban, I.; Žemva, B.; Bartlett, N. *Inorg. Chem.* **1989**, *28*, 3467.
(5) Sharpe, A. G. *J. Chem. Soc.* **1949**, 2901.
(6) Engelmann, U.; Müller, B. G. *Z. Anorg. Allg. Chem.* **1991**, *598*, 103.
(7) Hoppe, R.; Homann, R. *Z. Anorg. Allg. Chem.* **1970**, *379*, 193.
(8) Žemva, B.; Hagiwara, R.; Casteel, W. J., Jr.; Lutar, K.; Jesih, A.; Bartlett, N. *J. Am. Chem.* Soc. **1990**, *112*, 4846.

10.1021/ic9905603 CCC: $18.00 
Published on Web 10/04/1999

The metal vacuum and fluorine handling line was also as described previously.[4] All solid starting materials and products were transferred and weighed within the dry argon atmosphere of a Vacuum Atmospheres Corp. DRILAB. X-ray powder diffraction photographs (XRDPs) were obtained as previously described,[8] as were magnetic measurements employing a SQUID.[9]

**Materials.** Anhydrous HF (aHF; Matheson) was first dried in an FEP tube containing $K_2NiF_6$ (Ozark-Mahoning Pennwalt, Tulsa, OK) and then in one containing $O_2AsF_6$. $O_2AsF_6$ was prepared by the method of Shamir and Binenboym.[10] $BF_3$ and $AsF_5$ (Ozark-Mahoning) were checked by IR spectroscopy to ensure absence of major impurities and then used as supplied. $AgF_2$ was prepared by the fluorination of AgF in aHF at ~20 °C. $AgFBF_4$ was prepared as previously described,[9] as were $O_2PtF_6$,[11] $O_2SbF_6$,[12] $O_2RuF_6$,[13] $AgAsF_6$,[9] $AgPtF_6$,[14] $XeF_5AgF_4$,[4] $AgBF_4$,[9] and $KAuF_4$.[15]

**Preparations. $AgAuF_4$ from $KAuF_4$ and AgF.** $KAuF_4$ (158.9 mg, 0.5092 mmol) was placed in one arm of a T-reactor and AgF (97.2 mg, 0.7662 mmol) in the other, and aHF (1.5 mL) was condensed in each limb. The $KAuF_4$ dissolved to a yellow solution but left a small brown residue, so this solution was decanted slowly, at 20 °C, into the colorless solution of the AgF to give a yellow precipitate in a colorless supernatant solution (indicating total precipitation of the $AuF_4^-$). The colorless solution was removed by decantation, and the yellow solid was washed (by back-distilled aHF) three times and vacuum-dried. An XRDP of the yellow diamagnetic solid (178.4 mg, 0.4685 mmol) showed only the pattern of $AgAuF_4$, which was indexed on the basis of a tetragonal unit cell with $a = 5.788(1)$ Å, $c = 10.806(2)$ Å, $V = 362.0(2)$ Å$^3$, and $Z = 4$ (see Table 1), and that of the solid from the decantate (82.5 mg) showed a complex pattern containing lines of $AgAuF_4$ and AgF.

**Attempts To Prepare $AgAuF_4$ and $AgAgF_4$ from $AF_3$ (A = Au, Ag) and AgF.** $AuF_3$ or $AgF_3$, each prepared from its $KAF_4$ salt,[16] was placed in one arm of a T-reactor and a large molar excess of AgF in the other. AgF dissolved in aHF was poured into the limb containing the $AF_3$ (A = Ag, Au) and the reactor agitated for more than 1 day at ~20 °C. The $AF_3$ (A = Ag, Au) was unchanged in appearance, as was the residual weight on removal of the AgF solution. An XRDP showed unchanged $AuF_3$; in the case of $AgF_3$, there was some conversion[16] to $Ag_3F_8$.

**Preparation of $Ag^IAg^{III}F_4$.** Various other attempts were made to synthesize $Ag^IAg^{III}F_4$, all carried out in aHF: (a) AgF + $KAgF_4$; (b) $XeF_5AgF_4$ + $AgBF_4$; (c) $AgBF_4$ + $KAgF_4$. Reaction (a) gave only $Ag^{II}F_2$ as did reaction (b). Although the insolubility of $Ag^IAg^{III}F_4$ and the low solubility of $AgBF_4$ in aHF rendered reaction (c) slow, it did provide $Ag^IAg^{III}F_4$ essentially free of $AgF_2$. The red-brown $Ag^IAg^{III}F_4$ was on one occasion observed to transform rapidly to light-ochre-colored $Ag^{II}F_2$ (the latter established subsequently by its characteristic XRDP), accompanied by vigorous boiling of the aHF, indicative of the exothermicity of that change. The details that follow are for a preparation which gave $Ag^IAg^{III}F_4$, the XRDP of which revealed only $AgBF_4$ contamination and no $Ag^{II}F_2$. SQUID measurements did exhibit a weak paramagnetism (shown in Figure 1) indicative of contamination by a trace of a weakly paramagnetic impurity, but this was not $Ag^{II}F_2$, since this is revealed by its characteristic field dependence[17] below 163 K. The very low values of $\chi_g$ suggest that the bulk of the material is diamagnetic. One arm of a T-reactor was loaded with $KAgF_4$ (111.3 mg, 0.499 mmol) and $AgBF_4$ (89.8 mg, 0.461 mmol), aHF (1.5 mL) was added, and the mixture was brought from −81 to +10 °C over ~24 h, with constant agitation. The yellow solution color ($AgF_4^-$) faded, and a homogeneous red-brown insoluble solid was produced. The supernatant solution (still pale yellow) was decanted to the other limb and the aHF removed under vacuum. No attempt was made to wash the red-brown residue. The composition of the products was computed on the assumption that all Ag(I) remained with the aHF-insoluble residue and that all $K^+$ transferred with the decanted solution. Found, red-brown residue (XRDP showed only a weak $AgBF_4$ pattern): 116.4 mg. Required: for 0.274 mmol of $Ag^IAg^{III}F_4$, 79.9 mg; for 0.188 mmol of $AgBF_4$, 36.5 mg; total, 116.4 mg. Found, as a pale yellow solid from the decanted solution (XRDP showing $KAgF_4$ and $KBF_4$): 86.4

**Table 1.** X-ray Powder Data (Debye−Scherrer Method, Cu Kα Radiation, Ni Filter) for $AgAuF_4$, Tetragonal Cell, with $a = 5.788(I)$ Å, $c = 10.806(2)$ Å, $V/Z = 90.49(5)$ Å$^3$

| | | $1/d^2 \times 10^4$ | | | | | $1/d^2 \times 10^4$ | | |
|---|---|---|---|---|---|---|---|---|---|
| $I_{calc}$[a] | $I/I_0$ | obs | calc | *hkl* | $I_{calc}$[a] | $I/I_0$ | obs | calc | *hkl* |
| *b* | vvw | 199 | | | 8 | ms | 7736 | 7340 | 244 |
| 5 | vw | 345 | 343 | 002 | 4 | mw | 7885 | 7869 | 228 |
| 9 | w | 596 | 597 | 110 | 8 | m | 8119 | 8104 | 512 |
| 100 | vvs | 944 | 940 | 112 | 3 | w | 8476 | 8456 | 336 |
| 30 | ms | 1197 | 1194 | 200 | 3 | w | 9167 | 9161 | 1110 |
| 8 | m | 1376 | 1370 | 004 | 2 | vw | 9545 | 9552 | 440 |
| 3 | vw | 1538 | 1537 | 202 | 2 | vw | 10243 | 10257 | 408 |
| 2 | vvw | 1585 | 1578 | 211 | 6 | m, *br*[c] | 10511 | 10492 | 532 |
| *b* | vvw | 1644 | | | 6 | w | 10868 | 10844 | 156 |
| 1 | vww | 1955 | 1967 | 114 | 3 | w | 10941 | 10922 | 444 |
| 1 | vvw | 2242 | 2263 | 213 | 7 | m, *br* | 11478 | 11451 | 248 |
| 14 | ms | 2386 | 2388 | 220 | 6 | m, *br* | 11566 | 11549 | 1310 |
| 28 | vs | 2567 | 2564 | 204 | 3 | vw | 11959 | 11940 | 620 |
| 1 | vvw | 2741 | 2741 | 222 | 2 | vw | 12134 | 12116 | 604 |
| 13 | ms | 3692 | 3680 | 116 | 1 | vvw | 12343 | 12332 | 0012 |
| 12 | ms | 3770 | 3758 | 224 | 7 | mw | 13251 | 13232 | 356 |
| 3 | vw | 4357 | 4355 | 134 | 8 | m | 13337 | 13310 | 264 |
| 3 | w | 4789 | 4776 | 400 | 4 | vw | 13531 | 13526 | 2012 |
| 1 | vvw | 5365 | 5373 | 330 | 4 | vw | 13954 | 13937 | 3310 |
| 2 | vw | 5480 | 5481 | 008 | 4 | vw | 14722 | 14720 | 2212 |
| 7 | w | 5723 | 5716 | 332 | 6 | w | 15043 | 15033 | 448 |
| 7 | mw | 5974 | 5970 | 420 | 11 | ms | 15280 | 15268 | 172 |
| 12 | m | 6070 | 6068 | 136 | 5 | ms | 15280 | 15268 | 552 |
| 8 | mw, *br* | 6132 | 6146 | 404 | 5 | vww | 15529 | 15522 | 640 |
| 1 | vvw | 6301 | 6313 | 422 | 11 | vw, *br* | 16226 | 16227 | 608 |
| 4 | mw | 6689 | 6675 | 208 | 19 | mw, *br* | 16324 | 16325 | 1510 |

[a] $I_{calc}$ placed the atoms in the following positions of space group *I*4/*mcm* (140):

| | *x* | *y* | *z* |
|---|---|---|---|
| Ag | 0 | 0 | 1/4 |
| Au | 0 | 1/2 | 0 |
| F | 0.1688 | 0.1688 | 0.8768 |

Atom positions were obtained from synchrotron powder diffraction data (Graudejus, O.; Bartlett, N. *To be Published*). [b] Impurity line. [c] br: broad.

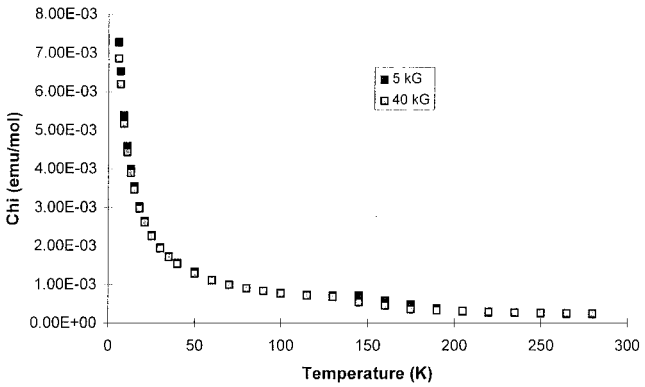


**Figure 1.** Molar susceptibility, $\chi_M$, versus *T* (K) for $Ag^IAg^{III}F_4$ admixed with $AgBF_4$.


(9) Casteel, W. J., Jr.; Lucier, G.; Hagiwara, R.; Borrmann, H.; Bartlett, N. *J. Solid State Chem.* **1992**, *96*, 84.
(10) Shamir, J.; Binenboym, J. *Inorg. Chim. Acta* **1968**, *23*, 101.
(11) Bartlett, N.; Lohmann, D. H. *J. Chem. Soc.* **1962**, 5253.
(12) McKee, D. E.; Bartlett, N. *Inorg. Chem.* **1973**, *12*, 2738.
(13) Edwards, A. J.; Falconer, W. E.; Griffiths, J. E.; Sunder, W. A.; Vasile, J. *J. Chem. Soc., Dalton Trans.* **1974**, 1129.
(14) Graudejus, O.; Elder, S. H.; Lucier, G. M.; Shen, C.; Bartlett, N. *Inorg. Chem.* **1999**, *38*, 2503−2509.
(15) Lucier, G.; Elder, S. H.; Chacón, L.; Bartlett, N. *Eur. J. Solid State Inorg. Chem.* **1996**, 33.
(16) Žemva, B.; Lutar, K.; Jesih, A.; Casteel, W. J., Jr.; Wilkinson, P.; Cox, D. E.; Von Dreele, R. B.; Borrmann, H.; Bartlett, N. *J. Am. Chem. Soc.* **1991**, *113*, 4192.
(17) Gruner, E.; Klemm, W. *Naturwissenschaften* **1937**, *25*, 59. Charpin, P.; Diamoux, A. J.; Marquet-Ellis, H.; Nguyen-Nghi. *C. R. Acad. Sci.* **1967**, *264*, 1108.

mg. Required: for 0.274 mmol of $KBF_4$, 34.5 mg; for 0.225 mmol of $KAgF_4$, 50.3 mg; total, 84.8 mg.

**Disproportionation of $AgFAsF_6$ in aHF.** $AgFAsF_6$ (~600 mg) in one limb of a T-apparatus was treated with an aliquot (~1 mL) of aHF, to give a blue solution (akin to that formed when $AgF_2$ and $AsF_5$ in a 1:2 molar ratio dissolve in a small amount of aHF) and a black solid. The blue solution was decanted from the black solid, and the aHF and $AsF_5$ were removed under vacuum. A fresh aliquot of aHF, added to the $AgFAsF_6$ retrieved from the decantate, again produced an insoluble black solid, which by successive rinsings and decantations was added to the original solvolysis product, the blue solution again separated from the mixture, and the remaining $AgFAsF_6$ was recovered as before. This was repeated several times until most of the $AgFAsF_6$ had been solvolyzed. Toward the end, it became apparent that the black solid was accompanied by a colorless solid which sedimented more slowly than the black solid in the aHF solution and so formed an upper layer in the sediment. XRDPs of the mixed solid product revealed that it contained[18] $AgAsF_6$ (the colorless solid) and showed a pattern akin to that of a trifluoride, such as[19] $RuF_3$ (this was characteristic of the black solid). It was found that oxidation of the $AgFAsF_6$ with $O_2AsF_6$ or with $F_2$ in aHF at ~20 °C left the black solid uncontaminated by a second phase. It was also noted that when the black solid was exposed to aHF containing $AsF_5$, $AgF_3$ was released. That, and the preparation of $AgF_4^-$ salts from the black solid with alkali-metal fluorides, suggested that the black solid contained $AgF_4^-$. The pseudo*trifluoride* nature of the black solid and various gravimetries for high-yield syntheses (see below) indicated the composition $Ag_3AsF_{12}$.

**Interaction of $AgFAsF_6$ with Massive aHF.** The disproportionation of $AgFAsF_6$ to $AgAsF_6$ and $Ag_3AsF_{12}$ just described does not hold if a large multimolar excess of aHF is added to the $AgFAsF_6$ (i.e., when the $AsF_5$ concentration in the aHF from the solvolysis is very low). Under those circumstances, the solid product is largely $AgF_2$.

**Quantitative Oxidation of $AgAsF_6$ to $AgFAsF_6$ by $O_2AsF_6$, at ~20 °C.** A T-reactor was loaded with $AgAsF_6$ (128.8 mg, 0.4340 mmol) in the main tube and with $O_2AsF_6$ (100.1 mg, 0.4531 mmol) in the sidearm, and aHF (dried first with $K_2NiF_6$ and then with $O_2AsF_6$) was distilled (1.5 mL) onto each solid. The $O_2AsF_6$ solution was poured, in several batches, into the suspension of $AgAsF_6$ at ~20 °C. The mixture evolved $O_2$ and gave an intense blue solution as the mixing proceeded, and all solid $AgAsF_6$ was consumed. Removal of volatiles in vacuo

($\leq 10^{-3}$ Torr) left a blue-green solid, the XRDP of which indicated[9,20] only the pattern of $AgFAsF_6$. Product weight: 145.5 mg; 0.434 mmol $AgFAsF_6$ requires 137 mg. (Some loss of container weight, resulting in apparent higher product mass, often occurs when $O_2^+$ and $F_2$ are used in the oxidations.)

**Preparation of $Ag_3AsF_{12}$.** This black aHF-insoluble solid was prepared in several ways: (1) by the fluorination of $AgFAsF_6$ in aHF; (2) by oxidation, using $O_2AsF_6$, of (a) $AgF_2$, (b) $AgFAsF_6$, or (c) $AgFBF_4$. The methods in (2) were used in the $Ag_3MF_{12}$ (M = Sb, Au, Pt, Ru) preparations. Route 2a provided the compound $Ag_3AsF_{12}$ in high purity and yield: $AgF_2$ (69.3 mg, 0.475 mmol) and $O_2AsF_6$ (36.8 mg, 0.167 mmol) were loaded respectively into the sidearm and the main tube of a prepassivated T-shaped Teflon-FEP reactor. Some aHF (~1.5 mL), dried over $O_2AsF_6$ in a separate FEP reactor, was transferred to the $AgF_2$ and to the $O_2AsF_6$. The $O_2AsF_6$ solution was poured slowly into the $AgF_2$ suspension. Oxygen evolution was immediately observed, and a black solid was produced. This mixture was agitated for ~30 min. Then the supernatant solution was decanted into the main tube and the black solid was washed with back-distilled aHF (five times) to the point where the black solid no longer settled quickly but remained several minutes in suspension in the aHF. This was the signal that soluble salts had been largely removed. All volatiles were removed under a dynamic vacuum ($\leq 10^{-3}$ Torr). The XRDP showed only the pseudotrifluoride pattern which was completely indexed on the basis of a primitive monoclinic cell (see Table 2). The weight of black solid was 95 mg; that expected for 0.1584 mmol of $Ag_3AsF_{12}$ was 99.2 mg.

**Table 2.** X-ray Powder Data (Debye−Scherrer Method, Cu Kα Radiation, Ni Filter) for $Ag_3AsF_{12}$[a]

| | | $1/d^2 \times 10^4$ | | | | | $1/d^2 \times 10^4$ | | |
|---|---|---|---|---|---|---|---|---|---|
| $I/I_0$ | $I_{calc}$ | obs | calc | *hkl* | $I/I_0$ | $I_{calc}$ | obs | calc | *hkl* |
| ms | 53 | 671 | 665 | 002 | w | 2 | 6160 | 6161 | 330 |
| s | 100 | 692 | 685 | 110 | vw | 1 | 6245 | 6253 | 402 |
| ms | 36 | 1252 | 1243 | 112 | w | 3 | 6358 | 6352 | 116 |
| m | 18 | 1295 | 1290 | 200 | w | 4 | 6449 | 6453 | 134 |
| ms | 10 | 1459 | 1448 | 020 | w | 3 | 6449 | 6455 | 042 |
| ms | 18 | 1459 | 1456 | 112 | vw | 3 | 6489 | 6507 | 332 |
| vvw | 2 | 1646 | 1652 | 210 | unobs | 3 | | 6565 | 314 |
| vw | 3 | 1748 | 1743 | 202 | vw | 3 | 6604 | 6609 | 420 |
| vvw | 2 | 1784 | 1770 | 120 | vvw | 1 | 6632 | 6639 | 206 |
| vw, *br*[b] | 4 | 1882 | 1859 | 013 | vw | 3 | 6845 | 6849 | 422 |
| vw, *br* | 4 | 1882 | 1883 | 121 | w | 2 | 6971 | 6972 | 404 |
| vw | 4 | 1927 | 1925 | 211 | w | 2 | 6971 | 6991 | 116 |
| m | 14 | 2117 | 2113 | 022 | vw | 3 | 7070 | 7081 | 240 |
| w | 8 | 2172 | 2168 | 202 | vw | 2 | 7116 | 7145 | 332 |
| vvw | | 2247 | | imp? | vvw | 0 | 7313 | 7309 | 043 |
| mw | 7 | 2669 | 2661 | 004 | vw | 3 | 7435 | 7434 | 026 |
| ms | 14 | 2746 | 2738 | 220 | vw | 3 | 7540 | 7533 | 242 |
| m | 14 | 3142 | 3133 | 114 | vw | 3 | 7674 | 7700 | 422 |
| m | 13 | 3202 | 3190 | 222 | w, *br* | 2 | 7954 | 7916 | 206 |
| m | 14 | 3267 | 3265 | 310 | w, *br* | 3 | 7954 | 7959 | 242 |
| mw, *br* | 3 | 3573 | 3526 | 204 | vw | 2 | 8077 | 8087 | 226 |
| mw, *br* | 7 | 3573 | 3558 | 114 | vvw | 2 | 8165 | 8183 | 334 |
| mw, *br* | 8 | 3573 | 3580 | 130 | vww | 1 | 8282 | 8316 | 316 |
| ms | 7 | 3621 | 3611 | 312 | w, *br* | 1 | 8411 | 8419 | 424 |
| ms | 6 | 3621 | 3616 | 222 | w, *br* | 2 | 8411 | 8427 | 510 |
| mw, *br* | 7 | 4134 | 4108 | 024 | w, *br* | 2 | 8411 | 8451 | 044 |
| mw, *br* | 6 | 4134 | 4138 | 132 | wv, *br* | 2 | 9346 | 9316 | 244 |
| w | 6 | 4235 | 4250 | 312 | wv, *br* | 1 | 9346 | 9363 | 226 |
| m, *br* | 9 | 4358 | 4351 | 132 | wv, *br* | 2 | 9346 | 9370 | 150 |
| m, *br* | 5 | 4358 | 4377 | 204 | vw | 1 | 9608 | 9625 | 512 |
| mw | 6 | 4976 | 4973 | 224 | wv, *br* | 1 | 9891 | 9872 | 406 |
| vw | 3 | 5148 | 5162 | 400 | wv, *br* | 2 | 9891 | 9886 | 136 |
| mw | 4 | 5300 | 5288 | 314 | wv, *br* | 2 | 9891 | 9929 | 152 |
| vw | 2 | 5409 | 5402 | 402 | vww, *br* | 2 | 10018 | 10024 | 514 |
| m | 1 | 5812 | 5790 | 040 | wv, *br* | 2 | 10156 | 10121 | 424 |
| m | 3 | 5812 | 5824 | 224 | wv, *br* | 2 | 10156 | 10141 | 152 |
| w, *br* | 1 | 6008 | 5087 | 006 | vw, *br* | 2 | 10156 | 10167 | 244 |
| w, *br* | 2 | 6008 | 134 | | | | | | |

[a] The calculated $1/d^2$ values and intensities of reflections are based on the parameters obtained from the structure analysis on a perfectly disordered single crystal: $a = 5.6045(6)$ Å, $b = 5.2567(6)$ Å, $c = 7.8061(8)$ Å, $\beta = 96.594(9)°$, $V = 228.5(8)$ Å$^3$, $Z = 1$, space group $P2/c$. [b] br: broad.

**Preparation of $Ag_3PtF_{12}$ from the Interaction of $O_2PtF_6$ with $AgFBF_4$ in aHF.** The experimental arrangement was like that for $Ag_3AsF_{12}$, the salt $AgFBF_4$ (58.3 mg, 0.2728 mmol) in the place of the $AgF_2$ and $O_2PtF_6$ (100.3 mg, 0.2941 mmol) in the place of $O_2AsF_6$. The $O_2PtF_6$ (in ~1.5 mL of aHF) partly in solution, and the remainder in the slurried suspension, was added in small portions to the stirred suspension of the $AgFBF_4$ (in ~1.5 mL of aHF). Immediately the precipitation of a nearly black solid (having a dark red reflectance) was observed. The mixture was agitated at ~20 °C for 30 min, and the yellow supernatant solution (containing the excess $O_2PtF_6$) was decanted to the other limb. The nearly black solid was washed with back-distilled aHF until the washings were free of color and then vacuum-dried ($\leq 10^{-3}$ Torr). The XRDP (see Table 3) was complex and indicated the presence of $Ag^{II}Pt^{IV}F_6$ as well as an $Ag_3AsF_{12}$-like phase. The data were indexed on a monoclinic cell akin to that of $Ag_3AsF_{12}$ for the dominant phase, the remaining lines then being largely due to the rhombohedral cell[14] of the $Ag^{II}Pt^{IV}F_6$. The insoluble solid weighed 81.7 mg. Required for conversion of all Ag(II) to equimolar quantities of the two products: for 0.0682 mmol of $AgPtF_6$, 28.3 mg; for 0.0682 mmol of $Ag_3PtF_{12}$, 50.8 mg; total, 79.1 mg.

**Preparation of $Ag_3AuF_{12}$ from $O_2AuF_6$ and $AgF_2$ in Acidified aHF.** With arrangements similar to those used for the synthesis of $Ag_3$-

(18) Kemmitt, R. D. W.; Russell, D. R.; Sharp, D. W. A. *J. Chem. Soc.* **1963**, 4408.
(19) Casteel, W. J., Jr.; Wilkinson, A. P.; Borrmann, H.; Serfass, R. E.; Bartlett, N. *Inorg. Chem.* **1992**, *31*, 3124.
(20) Gantar, D.; Frlec, B.; Russell, D. R.; Holloway, J. H. *Acta Crystallogr., Sect. C: Cryst. Struct. Commun.* **1987**, *C43*, 618.

**Table 3.** X-ray Powder Data (Debye−Scherrer Method, Cu Kα Radiation, Ni Filter) for $Ag_3PtF_{12}$, Monoclinic Cell with $a = 5.69(1)$ Å, $b = 5.25(1)$ Å, $c = 7.81(1)$ Å, $\beta = 97.7(1)°$, $Z = 1$, $V = 231(1)$ Å$^3$, Possible Space Group $P2/c$

| | | $1/d^2 \times 10^4$ | | | | | $1/d^2 \times 10^4$ | | |
|---|---|---|---|---|---|---|---|---|---|
| $I/I_0$ | $I_{calc}$[a] | obs | calc | *hkl* | $I/I_0$ | $I_{calc}$[a] | obs | calc | *hkl* |
| vw | | 574 | | | ms | | 2267 | | |
| vw | | 603 | | | vw | 7 | 2671 | 2673 | 004 |
| vs | 51 | 668 | 668 | 002 | ms | 14 | 2714 | 2710 | 220 |
| | 100 | 668 | 677 | 110 | vw, *br*[b] | | 2792 | | |
| w | | 707 | | | vw | | 2928 | | |
| w | | 737 | | | ms | 14 | 3099 | 3105 | $11\bar{4}$ |
| vw | | 784 | | | ms | 13 | 3099 | 3135 | $22\bar{2}$ |
| vvw | 3 | 1031 | 1031 | $01\underline{2}$ | ms | 14 | 3181 | 3194 | 310 |
| s | 39 | 1220 | 1223 | $11\bar{2}$ | vw, *br*[b] | | 3255 | | |
| *s*[b] | 19 | 1272 | 1258 | 200 | w | 7 | 3503 | 3494 | $31\bar{2}$ |
| vw | | 1371 | | | ms | 8 | 3577 | 3580 | 130 |
| s | 12 | 1452 | 1451 | 020 | ms | 7 | 3577 | 3596 | 114 |
| s | 20 | 1452 | 1468 | 112 | vw | | 3805 | | |
| ms, *br*[b,c] | | 1564 | | | ms | 7 | 4131 | 4125 | $02\underline{4}$ |
| ms, *br* | 4 | 1680 | 1681 | $20\bar{2}$ | ms | 6 | 4131 | 4125 | $13\bar{2}$ |
| vw, *br* | 2 | 1858 | 1865 | $01\underline{3}$ | vw | 6 | 4235 | 4231 | 312 |
| vw, *br* | 3 | 1858 | 1871 | $12\bar{1}$ | ms | 8 | 4370 | 4371 | 132 |
| vw, *br* | 2 | 1962 | 1911 | 211 | vvw | | | 4669 | |
| ms | 16 | 2119 | 2120 | 022 | vvw | | 4835 | | |
| vw | 8 | 2183 | 2172 | 202 | vvw | 4 | 5118 | 5130 | $31\bar{4}$ |

[a] Calculated using the Parameters from $(AgF)_2AgF_4AsF_6$ single-crystal analysis. [b] These lines, or contributions to them, are attributable to $Ag^{II}Pt^{IV}F_6$ (ref 14). [c] br: broad.

**Table 4.** X-ray Powder Data (Debye−Scherrer Method, Cu Kα Radiation, Ni Filter) for $Ag_3AuF_{12}$, Monoclinic Cell with $a = 5.66(1)$ Å, $b = 5.24(1)$ Å, $c = 7.79(1)$ Å, $\beta = 97.5(1)°$, $Z = 1$, $V = 229(1)$ Å$^3$, Possible Space Group $P2/c$

| | | $1/d^2 \times 10^4$ | | | | | $1/d^2 \times 10^4$ | | |
|---|---|---|---|---|---|---|---|---|---|
| $I/I_0$ | $I_{calc}$[a] | obs | calc | *hkl* | $I/I_0$ | $I_{calc}$[a] | obs | calc | *hkl* |
| m | 51 | 675 | 671 | 002 | w | 4 | 3471 | 3470 | $20\bar{4}$ |
| vs | 100 | 686 | 682 | $11\underline{0}$ | w | 7 | 3533 | 3531 | $31\bar{2}$ |
| s | 39 | 1233 | 1232 | $11\bar{2}$ | s, *br*[b] | 8 | 3610 | 3595 | 130 |
| w | 19 | 1268 | 1270 | 200 | s, *br* | 7 | 3610 | 3608 | 114 |
| s | 12 | 1463 | 1457 | 020 | s, *br* | 7 | 3610 | 3640 | 22 |
| s | 20 | 1463 | 1474 | $11\underline{2}$ | m, *br* | 7 | 4138 | 4141 | $02\underline{4}$ |
| vvw | 4 | 1703 | 1699 | $20\bar{2}$ | m, *br* | 6 | 4138 | 4145 | $13\bar{2}$ |
| vvw | 2 | 1884 | 1874 | $01\underline{3}$ | w, *br* | 6 | 4270 | 4257 | 312 |
| vvw | 2 | 1884 | 1882 | $12\bar{1}$ | s, *br* | 8 | 4398 | 4387 | 132 |
| m | 16 | 2126 | 2128 | 022 | s, *br* | 4 | 4398 | 4439 | $20\underline{4}$ |
| vw | 8 | 2186 | 2184 | 202 | m, *br* | 6 | 4927 | 4927 | $22\bar{4}$ |
| w | 7 | 2684 | 2684 | 004 | vw, *br* | 3 | 5056 | 5082 | $40\underline{0}$ |
| s | 14 | 2720 | 2727 | $22\underline{0}$ | w, *br* | 4 | 5190 | 5181 | $31\bar{4}$ |
| s | 14 | 3123 | 3124 | $11\bar{4}$ | w, *br* | 3 | 5873 | 5895 | 224 |
| s | 13 | 3159 | 3156 | $22\bar{2}$ | w, *br* | 2 | 6126 | 6136 | $33\underline{0}$ |
| m | 14 | 3224 | 3223 | 310 | w, *br* | 3 | 6330 | 6358 | $11\bar{6}$ |

[a] Calculated using the parameters from $(AgF)_2AgF_4AsF_6$ single-crystal analysis. [b] br: broad.

$AsF_{12}$, $AgF_2$ (143.2 mg, 0.982 mmol) in aHF (∼2 mL) was shaken slowly into a solution of $O_2AuF_6$ (145.8 mg, 0.425 mmol) dissolved in aHF (∼2 mL), to which $BF_3$ (∼0.14 mmol) had been added to aid in the solubilization of the $AgF_2$ [as $Ag^{2+}(BF_4^-)_2$]. As the $AgF_2$ made contact with the yellow $O_2AuF_6$ solution, $O_2$ was evolved and a black solid precipitated. In the washing of the $AgF_2$ residue from the sidearm with cold back-distilled aHF containing $BF_3$, the characteristic blue color of dissolved Ag(II) was observed, but this rapidly dissipated on pouring into the yellow $AuF_6^-$ solution. The mixture was agitated for 12 h, and the excess $O_2AuF_6$ in the supernatant solution was decanted and washed over to the sidearm. The XRDP of the black solid showed an $Ag_3AsF_{12}$ type pattern, which was fully indexed on a monoclinic cell of that type (see Table 4), and that of the orange solid from the decantate proved it to be $O_2AuF_6$. The observed weight of $Ag_3AuF_{12}$ was 244.7 mg; 0.327 mmol of $Ag_3AuF_{12}$ requires 244.9 mg. The observed residue of $O_2AuF_6$ was 39.6 mg, which in excess should have been 33.6 mg.

**$Ag_3RuF_{12}$ and $Ag_3SbF_{12}$ Preparations.** These were carried out in essentially the same manner as that of $Ag_3PtF_{12}$, using $AgFBF_4$ and the appropriate $O_2^+MF_6^-$ salt. The XRDP data for each product are given in Tables S1 and S2, respectively (Supporting Information).

**$Ag_3MF_{12}$ Salts with Alkali-Metal Fluorides in aHF.** The salts interact with alkali-metal fluorides (AFs) in aHF to generate a solution of the $AAgF_4$ and $AMF_6$ (A = Li has highest solubility, and A = Cs, the least) and an insoluble residue of $AgF_2$. The interaction of $Ag_3AsF_{12}$ with KF is representative. A solution of KF (25.5 mg, 0.439 mmol) in aHF in the sidearm of a T-reactor was poured onto a suspension of $Ag_3AsF_{12}$ (111 mg, 0.177 mmol) in aHF (1.5 mL) at ∼20 °C. The black solid was immediately converted to a yellow solution and a brown insoluble residue. The XRDP of the yellow solid from the decantate showed the pattern of $KAgF_4$ strongly, lines characteristic of $KAsF_6$ and $KHF_2$ also being present. The brown residue was $AgF_2$.

**Single-Crystal Growth of $Ag_3AsF_{12}$.** The reaction vessels for crystal growth were usually constructed of $^3/_8$ in. FEP tubing, Teflon tees, and Teflon valves with Kel-F stems and Teflon tips. A restriction, ∼1 cm away from the sealed end of the sidearm, was made by pinching the FEP tubing under heat to less than half its diameter. The purpose of this was to slow the diffusion of $F_2$ during crystal growth. Typically, $AgFAsF_6$ was loaded into the main arm of the FEP reactor, the other starting material, either $AgF_2$ or $AgFBF_4$ (in slight molar deficit of the $AgFAsF_6$), was loaded into the sidearm, and aHF (1−2 mL) was condensed onto the $AgFAsF_6$. This gave a blue solution and a small amount of black solid. After the black solid had settled, the blue solution was carefully decanted onto the solid in the sidearm. $F_2$ was then admitted into the reactor until the total pressure was about 1000 Torr. The reactor was then left undisturbed for about 1 week for crystal growth from this solution. During crystal growth, the blue solution usually became much paler; meanwhile, the initial $AgF_2$ or $AgFBF_4$ slowly diminished as highly reflective black crystallites grew, from solution, on the reactor wall. At the end of the crystal growth, the solution was carefully decanted back into the main tube, to leave the crystals on the sidearm wall, from which they were retrieved (in the DRILAB) after the system had been vacuum-dried ($10^{-3}$ Torr) for several hours.

The multifaceted, highly reflective, jet black $(AgF_2)_3AsF_6$ crystallites were roughly cubical. They were usually very small, tended to form aggregates, and were usually twinned. The most satisfactory batch, from which a suitable single crystal of $(AgF_2)_3AsF_6$ was obtained, was from the reaction of $AgFBF_4$, $AgFAsF_6$, and $F_2$ with a small amount of $KBF_4$ present in the aHF.

**Crystal Structure Determination of $Ag_3AsF_{12}$.** Crystals were manipulated under a dry argon atmosphere in the DRILAB on a prepassivated Teflon sheet. The selected crystal was mounted in a 0.5 mm diameter quartz capillary, the narrow end of which had been further drawn down to a long taper. Preliminary Laue and precession photographs indicated monoclinic Laue symmetry and yielded cell dimensions close to those derived from the X-ray powder data (see Table 2).

The crystal used for data collection was transferred to an Enraf-Nonius CAD-4 diffractometer. Automatic peak search and indexing procedures yielded the same monoclinic cell as derived from the X-ray powder diffraction data and precession photographs. Testing showed that the cell was indeed primitive and that there was no superlattice present. Table 5 gives the crystal data and X-ray experimental parameters, and Table 6, the interatomic distances and angles. Positional and thermal parameters are given in Table S3 (Supporting Information).

A total of 1463 raw intensity data were collected. Inspection of the azimuthal scan data showed a variation of $I_{min}/I_{max} = 0.82$ for the average curve. An empirical correction based on the observed variation was applied to the data as a first approximation. The structure was solved by Patterson methods in space group $P\bar{1}$. Refinement and elucidation of additional atoms proceeded via standard least-squares and Fourier techniques.[21] Examination of the triclinic model demonstrated the correct monoclinic space group, $P2/c$ (the apparent absence of $h0l$, $l \neq 2n$ has been found), and refinement continued in that group

(21) *MolEN-1990*; Delft Instruments, X-ray Diffraction D.V.: Rontgenweg 1, 2624 BD Delft, The Netherlands, 1990.

**Table 5.** Crystal and Data Parameters for $Ag_3AsF_{12}$

| | |
|---|---|
| formula | $Ag_3AsF_{12}$ |
| fw | 626.5 |
| space group | $P2/c$ |
| $a$/Å | 5.6045(6) |
| $b$/Å | 5.2567(6) |
| $c$/Å | 7.8061(8) |
| $\beta$ (deg) | 96.594(9) |
| $V$/Å$^3$ | 228.5(8) |
| $Z$ | 1 |
| $T$/K | 298 |
| $\rho_{calcd}$/g cm$^{-3}$ | 100.6 |
| radiation, $\lambda$/Å | 0.710 73 (Mo K$\alpha$) |
| reflns measd | $\pm h, +k \pm l$ |
| residuals | $R^a = 2.44$; $R_w{}^b = 2.89$ |

[a] $R = \sum||F_o| - |F_c||/\sum|F_o|$. [b] $R_w = [\sum w(|F_o| - |F_c|)^2/\sum wF_o{}^2]^{1/2}$.

**Table 6.** Crystal and Data Parameters for $Ag_3AsF_{12}$

| | | | |
|---|---|---|---|
| As/Ag2−F2 | 1.80(2) | Ag1−F1 | 2.003(4) |
| As/Ag2−F3 | 1.81(2) | Ag1−F2 | 2.34(2) |
| As−F4 | 1.72(3) | Ag1−F3 | 2.32(2) |
| Ag2−F4 | 2.61(3) | | |
| F2−F3 | 2.51(3) | F2−F3 | 2.59(3) |
| F2−F4 | 2.36(4) | F2−F4 | 2.62(3) |
| F3−F4 | 2.38(3) | F3−F4 | 2.60(3) |
| F1−F2 | 3.19(2) | F1−F2 | 2.96(3) |
| F1−F3 | 3.01(2) | F1−F3 | 3.12(2) |
| F1−F4 | 3.14(3) | F1−F4 | 3.09(3) |
| F2−F2 | 2.98(3) | F2−F3 | 3.22(3) |
| F2−F3 | 3.11(3) | F2−F4 | 3.26(3) |
| F2−F4 | 3.09(3) | F3−F3 | 3.16(4) |
| F3−F3 | 3.02(4) | F3−F4 | 3.08(3) |
| F3−F4 | 3.09(4) | F3−F4 | 3.26(3) |

| | | | |
|---|---|---|---|
| F1−Ag1−F1 | 180 | F1−Ag1−F2 | 94.4(6) |
| F1−Ag1−F2 | 85.6(6) | F1−Ag1−F3 | 87.8(5) |
| F1−Ag1−F3 | 92.2(5) | F2−Ag1−F2 | 180 |
| F2−Ag1−F3 | 92.4(7) | F2−Ag1−F3 | 87.6(7) |
| F3−Ag1−F3 | 180 | F2−Ag2−F2 | 180 |
| F2−Ag2−F3 | 88.2(9) | F2−Ag2−F3 | 91.8(9) |
| F2−Ag2−F4 | 93.2(8) | F2−Ag2−F4 | 86.8(8) |
| F3−Ag2−F3 | 180 | F3−Ag2−F4 | 86.7(9) |
| F3−Ag2−F4 | 93.3(9) | F4−Ag2−F4 | 180 |
| F2−As−F2 | 180 | F2−As−F3 | 88.2(9) |
| F2−As−F3 | 91.8(9) | F2−As−F4 | 93.2(8) |
| F2−As−F4 | 86.8(8) | F3−As−F3 | 180 |
| F3−As−F4 | 86.7(9) | F3−As−F4 | 93.3(9) |
| F4−As−F4 | 180 | Ag1−F1−Ag1 | 154(2) |
| Ag1−F2−As/Ag2 | 136.0(9) | Ag1−F3−As/Ag2 | 137.2(9) |
| As−F4−Ag2 | 127(2) | | |

with a completely disordered model for Ag2 and the As and half-occupancy for F4 (that closest to As, along $c$).

After solution of the structure and assignment of the correct space group, an empirical correction[22] was applied to the data on the basis of the combined differences of $F_o$ and $F_c$ following refinement of all atoms with isotropic thermal parameters (corr(max) = 1.32, corr(min) = 0.79; no $\theta$ dependence). Removal of systematically absent data and averaging of redundant data ($R_I$ = 4.3% for observed data) left 670 unique data in the final data set.

The final residuals for 40 variables refined against the 213 data for which $F^2 > 2.5\sigma(F^2)$ were $R$ = 2.44%, $R_w$ = 2.89%, and GOF = 1.06. The $R$ value for all 670 data was 15.2%. (This very large value is in part an artifact of the way that reflections with negative measured intensities are treated in the calculation of $R_{all}$. In part it is due to the fact that only 15 0$kl$ and general $hkl$ reflections with $l = 2n + 1$ are "observed" in the data set.)

The quantity minimized by the least squares program was $\sum w(|F_o| - |F_c|)^2$. The $p$ factor, used to reduce the weight of intense reflections, was set to 0.03 throughout the refinement. The analytical forms of the scattering factor for the neutral atoms were used,[23] and all scattering factors were corrected for both the real and imaginary components of anomalous dispersion.[24]

Inspection of the residuals ordered in ranges of (sin $\theta$)/$\lambda$, $|F_o|$, and parity and values of the individual indexes showed no unusual features or trends, other than those caused by the strong pseudotranslation of $^1/_2c$ in the structure. There was no indication of secondary extinction in the high-intensity low-angle data.

## Results and Discussion

The favored disproportionation of silver in AgO to Ag(I) and Ag(III)[2] contrasts with the behavior of the mixed-oxidation-state fluoride $Ag^IAg^{III}F_4$, prepared in these studies, which undergoes exothermic conversion to $Ag^{II}F_2$:

$$Ag^IAg^{III}F_4 \rightarrow 2Ag^{II}F_2 \quad (3)$$

It was anticipated that $Ag^IAg^{III}F_4$, like Ag(I)Au(III)$F_4$, would have its square-planar anions arranged perpendicular to one another and all parallel to the $4_2$ axis of the $KBrF_4$ type structure observed in alkali-metal $AgF_4^-$ and $AuF_4^-$ salts[6,7] and, as found here, for $AgAuF_4$ (see Table 1). It was hoped that this simple symmetric structure would provide kinetic stability. With the synthetic approach used to obtain $Ag^IAg^{III}F_4$

$$Ag^IBF_4(c) + K^+(solv) + Ag^{III}F_4{}^-(solv) \xrightarrow{aHF,\ \le 0\ ^\circ C} Ag^IAg^{III}F_4(c) + K^+(solv) + BF_4{}^-(solv) \quad (4)$$

the mixed-valence red-brown solid was always noncrystalline, probably as a consequence of the small particle size associated with the insolubility of the material in aHF and its rather rapid generation at low temperatures [both deliberately employed to reduce the possibility of making the thermodynamically more favorable $Ag^{II}F_2$].

The thermodynamic stability of $Ag^{II}F_2$ does contrast with the failure to generate $AuF_2$ from $Au(SbF_6)_2$, that product[25] disproportionating to Au(0) and Au(III), i.e.

$$4Au^{2+}(solv) + 8F^-(solv) \xrightarrow{aHF} Au^{II}(Au^{III}F_4)_2(c) + Au(c) \quad (5)$$

and in highly basic aHF (with which $AgF_2$ does not react) Au(II) is completely converted to Au(III) and Au(0):

$$8F^-(solv) + 3Au^{II}(Au^{III}F_4)_2(c) \rightarrow 8AuF_4{}^-(solv) + Au(c) \quad (6)$$

This difference [represented by eq 1 contrasted with (5) and (6)] can be ascribed to a large relativistic effect at gold,[26−28] which enhances the binding of the Au s electrons and simultaneously (by the enhanced screening effect of the s electrons) causes the d electrons to be less bound. This effect causes metallic gold to be more strongly bonded than metallic silver and, at the same time, makes for easier oxidation of gold to Au(III) than of silver to Ag(III).

(22) Walker, N., Stuart, D. *Acta Crystallogr., Sect A* **1983**, *A39*, 159 (as used by the program DIFABS in MolEN).

(23) Cromer, D. T.; Waber, J. T. *International Tables for X-ray Crystallography*; The Kynoch Press: Birmingham, England, 1974; Vol. IV, Table 2.2.B.

(24) Cromer, D. T.; Waber, J. T. *International Tables for X-ray Crystallography*; The Kynoch Press: Birmingham, England, 1974; Vol. IV, Table 2.3.1.

(25) Elder, S. H.; Lucier, G. M.; Hollander, F. J.; Bartlett, N. *J. Am. Chem. Soc.* **1997**, *119*, 1020.

(26) Pitzer, K. *Acc. Chem. Res.* **1979**, *12*, 271.

(27) Pyykkö, P.; Desclaux, J.-P. *Acc. Chem. Res.* **1979**, *12*, 276.

(28) Pyykkö, P. *Chem. Rev.* **1988**, *88*, 563.

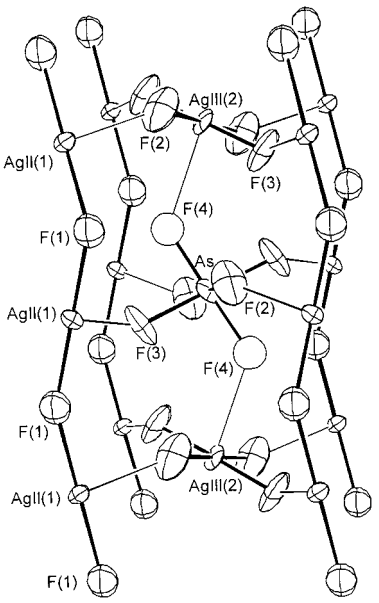


**Figure 2.** Ordered structural unit for the structure of $Ag_3AsF_{12}$. The ellipsoids are scaled to represent the 75% probability surface.

Although strongly basic aHF failed to disproportionate aHF-insoluble $Ag^{II}F_2$ (eq 1), it was found that dissolved Ag(II) would disproportionate in moderately acidic aHF. Precipitation of a black product, insoluble in aHF, was first noted in the studies of Žemva and co-workers[29] when 1 equiv of $AsF_5$ was added to $AgF_3$. An insoluble black solid was also produced when $AgFAsF_6$ was treated with fluorine in aHF or when (in an attempt at Berkeley to intercalate the puckered-sheet-structure of) $AgF_2$ was oxidized by $O_2^+AsF_6^-$. The black product of the last reaction was recognized as having a pseudotrifluoride XRDP, and the entire pattern was convincingly indexed on a monoclinic distortion of a rhombohedral trifluoride lattice.[30] This, in combination with gravimetry, eventually fixed the composition of the black solid as $Ag_3AsF_{12}$. Methods were then worked out for the slow generation of $Ag_3AsF_{12}$ from $AgF_2$, to produce single crystals. The most effective route was the slow fluorination of a blue solution of silver(II) fluoroarsenate (obtained by decantation from its solvolysis products—see below) in contact with either solid $AgF_2$ or solid $AgFBF_4$. The structure, illustrated in Figure 2, with interatomic distances and angles in Table 6, is in its essence, the salt $(AgF^+)_2AgF_4^-AsF_6^-$, the cations being chains akin to those first described by Gantar et al.[20] for $AgFAsF_6$ and those subsequently observed in a variety of $AgF^+$ salts from these laboratories.[9,31] The chain cations, running parallel to *c*, enclose stacks of alternating $AgF_4^-$ and $AsF_6^-$. An ordered stacking sequence of the anions is required, as adjacent $AsF_6^-$ would result in F4 ligand collision and repulsion of the anions. This would result in significant variation in the *z* parameters of the As and Ag2 atom positions, whereas the data fix the *z* parameters precisely. The ordered anion stacks, however, are not in registry with one another, and this renders all of the Ag(II) ions of the cation chains effectively equivalent. The observed As/Ag2−F distance (Table 6) of 1.81(2) Å is compatible with the average of Ag−F (in $KAgF_4$)[32] = 1.889(3) Å and As−F (in $KAsF_6$)[33] = 1.719(3) Å, which is 1.804 Å. The As−F4 distance of 1.72(3) Å is not significantly different from that expected for As(V)−F. It should be noted that the F-ligand bridging (including that of $AsF_6^-$ with $AgF_4^-$) from each anion to its four closest Ag(II) ions gives each Ag(II) or Ag(III) ion a distorted octahedral F-ligand environment, not much different from that of the $AsF_6^-$. This brings the $(AgF)_2AgF_4AsF_6$ structure close to that of the trifluoride structure[34] of $RhF_3$ or the pseudotrifluoride[35] $Pd^{II}Pd^{IV}F_6$.

It was found that relatives of $(AgF)_2AgF_4AsF_6$ could be prepared, with $AsF_6^-$ replaced by $MF_6^-$ (M = Sb, Ru, Pt, Au), the generally useful approach being to oxidize $AgF_2$ (solubilized in aHF with $BF_3$), or $AgFBF_4$, with the appropriate $O_2^+MF_6^-$ salts as oxidizers:

$$3AgF^+(solv) + 3BF_4^- + O_2^+(solv) + MF_6^-(solv) \xrightarrow{aHF} (AgF)_2AgF_4MF_6(c) + 3BF_3(g)(solv) + O_2(g) \quad (7)$$

The close similarity of their XRDPs and their unit cells (see Table 7) indicates that essentially the same pseudotrifluoride structure occurs in all of these materials.

The magnetic behavior of $(AgF)_2AgF_4AsF_6$ (see Figure 3) is very like that of $AgFAsF_6$ and indicates that the nearly temperature-independent paramagnetism is a property of the chain cation.[9,31] Although this is consistent with a partially filled band for the cation obedient to Fermi−Dirac statistics,[36] neither the anticipated Peierls distortion nor electrical conduction has ever been observed in these $(AgF)_n^{n+}$ systems. Even contacts to single crystals of $(AgF)_2AgF_4AsF_6$ with massive gold rods failed to find evidence of electrical conductance along the

**Table 7.** Comparison of Cell Dimensions for $Ag_3MF_{12}$ (M = As, Au, Pt, Sb, Ru)

| | $Ag_3AsF_{12}$ | $Ag_3AuF_{12}$[a] | $Ag_3PtF_{12}$[a] | $Ag_3SbF_{12}$[a] | $Ag_3RuF_{12}$[a] |
|---|---|---|---|---|---|
| *a* (Å) | 5.6045(6) | 5.66 | 5.69 | 5.70 | 5.67 |
| *b* (Å) | 5.2567(6) | 5.24 | 5.25 | 5.27 | 5.23 |
| *c* (Å) | 7.8061(8) | 7.79 | 7.81 | 7.83 | 7.80 |
| $\beta$ (deg) | 96.594(9) | 97.5 | 97.7 | 97.2 | 97.2(4) |
| *V* (Å$^3$) | 228.5(8) | 229 | 231 | 233 | 230(2) |

[a] The standard deviation being always 1 in the last digit unless otherwise noted.

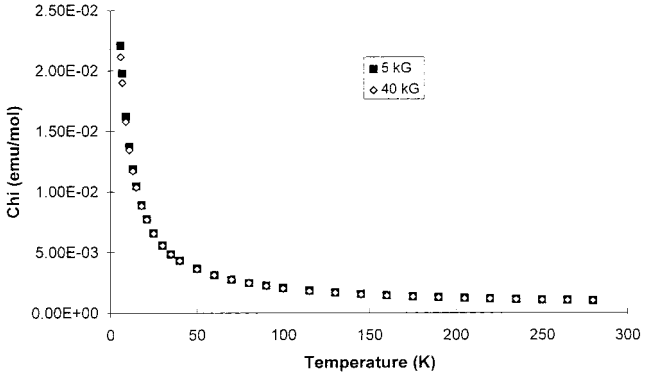


**Figure 3.** Molar susceptibility, $\chi_M$, versus *T* (K) for $Ag_3AsF_{12}$.

(29) Jesih, A.; Lutar, K.; Žemva, B. Unpublished observations, 1988.
(30) The original indexing of the pattern was achieved with a pseudotriclinic distortion of a trifluoride-like rhombohedral cell, with $a^{*2} = 0.0541$, $b^{*2} = c^{*2} = 0.0529$, $2a^*b^*\cos\gamma^* = 0.0386 = 2a^*c^*\cos\beta^*$, and $2b^*c^*\cos\alpha^* = 0.0390$, the equalities of which indicated the true monoclinic nature of the lattice.
(31) Lucier, G.; Munzenberg, J.; Casteel, W. J., Jr.; Bartlett, N. *Inorg. Chem.* **1995**, *34*, 2692.
(32) Lutar, K.; Milićev, S.; Žemva, B.; Müller, B. G.; Bachmann, B.; Hoppe, R. *Eur. J. Solid State Inorg. Chem.* **1991**, *28*, 1335.
(33) Grafner, G.; Kruger, G. J. *Acta Crystallogr., Sect. B* **1974**, *B30*, 250.
(34) Grosse, L.; Hoppe, R. *Z. Anorg. Allg. Chem.* **1987**, *552*, 123.
(35) Tressaud, A.; Winteberger, M.; Bartlett, N.; Hagenmuller, P. *C. R. Acad. Sci., Ser. C* **1976**, *282*, 1069.
(36) Kittel, C. *Introduction to Solid State Physics*; Wiley: New York, 1986; p 413.

expected conducting path (*c*). It must be pointed out, however, that even massive gold could be surface oxidized and fluorinated by such a powerful oxidizer,[31] and this could provide an insulating barrier.

Perhaps the most surprising aspect of $(AgF)_2AgF_4AsF_6$ is that it is sufficiently stable thermodynamically to drive the disproportionation of Ag(II) to Ag(I) and Ag(III), as $AgFAsF_6$ is solvolyzed by aHF:

$$4AgFAsF_6 \xrightarrow{\text{aHF limited}} AgAsF_6(c) + Ag_3AsF_{12}(c) + 2AsF_5(solv) \quad (8)$$

This occurs when the amount of added aHF is small and the resultant acidity ($AsF_5$ concentration) moderately high. A mixture of colorless $AgAsF_6$ and black $Ag_3AsF_{12}$ is formed. These solids sediment at different rates, the latter being more dense (4.55 versus 4.20 g $cm^{-3}$), resulting in the white solid depositing above the black in the aHF. Addition of fluorine or $O_2AsF_6$ (see below) to this mixture converts the $AgAsF_6$ to $AgFAsF_6$:

$$^1/_2F_2(g) + AgAsF_6(c) \xrightarrow{\text{aHF}} AgFAsF_6(c) \quad (9)$$

Thus, with these oxidizers present and the reaction of eq 8 repeated, all of the solid can be converted to $Ag_3AsF_{12}$. The interaction of $AgFAsF_6$ with a large excess of aHF (with the consequence that the acidity in $AsF_5$ is low) leads to simple solvolysis and $AgF_2$ production:

$$AgFAsF_6 \xrightarrow{\text{aHF large}} AgF_2(c) + AsF_5(solv) \quad (10)$$

Formation of $Ag_3AsF_{12}$ appears to be a consequence of the solvolytic disproportionation of $AgFAsF_6$, since oxidation of the blue solutions of $Ag^{2+}$(solv) does not generate it. Certainly the salt $O_2AsF_6$ does not interact with the blue solution in aHF prepared by adding two molar aliquots of $AsF_5$ to one of $AgF_2$. On the other hand, $O_2AsF_6$ rapidly and quantitatively oxidizes $AgAsF_6$ to such a blue solution, from which clear, blue-green $AgFAsF_6$ solution is recovered:[37]

$$AgAsF_6(c) + O_2^+(solv) + AsF_6^-(solv) \xrightarrow{\text{aHF}} Ag^{2+}(solv) + 2AsF_6^-(solv) + O_2(g) \quad (11)$$

The interaction of $AgAsF_6$ with $O_2PtF_6$ proceeds quite differently from (11), there being no significant $O_2$ evolution. Evidently the Ag(I) oxidation to Ag(II) is brought about by the $PtF_6^-$, which produces the insoluble $Ag^{II}Pt^{IV}F_6$ product, $O_2AsF_6$ being the aHF-soluble product:

$$AgAsF_6(c) + O_2^+(solv) + PtF_6^-(solv) \rightarrow AgPtF_6(c) + O_2^+(solv) + AsF_6^-(solv) \quad (12)$$

The different outcomes of the two reactions (eqs 11 and 12) probably stem from the anionic nature of the $PtF_6^-$ oxidizer, which must interact rapidly in its attractive encounter with $Ag^+$(solv) (from the slightly soluble $AgAsF_6$). Electron transfer to generate the close-packed pseudotrifluoride lattice[14] of $Ag^{2+}PtF_6^{2-}$ must occur immediately. The insolubility of this salt in aHF contributes to the simplicity of reaction 12.

(37) It should be noted that, at −80 °C (the solubility of $O_2$ in aHF then being higher and the $T\Delta S$ term for eq 11 much smaller), the reverse reaction is essentially complete; i.e., all $Ag^{2+}$(solv) is reduced to $AgAsF_6$(c) by $O_2$, which then precipitates as $O_2AsF_6$.

Reaction 1 may involve interaction of $Ag^+$(solv) with the solvated radical $O_2F$(solv) rather than with $O_2^+$(solv), since the weakness of the $O_2F$ base[38] and the merely moderate strength of $AsF_5$ as a $F^-$ acceptor[31] in the aHF solvent may mean that the $O_2AsF_6$ solution is not fully ionized:

$$O_2^+(solv) + AsF_6^-(solv) \overset{\text{aHF}}{\rightleftharpoons} O_2F(solv) + AsF_5(solv) \quad (13)$$

Attack on $Ag^+$(solv) by $O_2F$(solv) in the presence of $AsF_5$(solv) could then provide the observed $Ag^{2+}$(solv):

$$Ag^+(solv) + AsF_6^-(solv) + O_2F(solv) + AsF_5(solv) \xrightarrow{\text{aHF}} Ag^{2+}(solv) + 2AsF_6^-(solv) + O_2(g) \quad (14)$$

Removal of $AsF_5$ and aHF from this solution gives pure, blue-green $AgFAsF_6$, but as soon as aHF is added to this, the solvolytic disproportionation represented in eq 8 occurs. Neither reaction 11 nor reaction 12, however, gives a $Ag_3MF_{12}$ product. For formation of the latter, it appears to be necessary to disproportionate the $AgFMF_6$ salt.

In the interaction of $O_2PtF_6$ with $AgFBF_4$, the main product is the mixed-valence salt $(AgF)_2AgF_4PtF_6$, but $Ag^{II}Pt^{IV}F_6$ is a sizable byproduct that is easily detected in the XRDP of the products (see Table 3). If we assume that the generation of $Ag_3PtF_{12}$ requires the disproportionation of $AgFPtF_6$

$$4AgFPtF_6(c) + 2BF_4^- \rightarrow AgPtF_6(c) + Ag_3PtF_{12} + 2BF_3(g) + 2PtF_6^-(solv) \quad (15)$$

analogously to eq 8, $AgPtF_6$, which is[14] $Ag^{II}Pt^{IV}F_6$, should represent one-quarter of the initial $AgFBF_4$. $Ag^{II}Pt^{IV}F_6$, a salt of Ag(II) (probably as a result of its insolubility in aHF), does not interact with the dissolved $O_2^+$. The observed yields of $Ag_3PtF_{12}$ and $AgPtF_6$ are close to those expected on the basis of eq 15. This stands in contrast to the interaction of $AgFBF_4$ with $O_2AuF_6$, where $Ag_3AuF_{12}$ is produced free of $AgAuF_6$ (see Table 4).

The $AuF_6^-$(solv) species has a very stable $dt_{2g}^6$ electron configuration. Unlike $PtF_6^-$(solv), which has[14] an electron affinity ≥60 kcal $mol^{-1}$, $AuF_6^-$(solv) is not a strong one-electron oxidizer since its lowest lying empty orbital is of antibonding $\sigma$ character. In $PtF_6^-$(solv) on the other hand, the addition of an electron generates the filled-subshell $dt_{2g}^6$ species, $PtF_6^{2-}$(solv). When, therefore, the disproportionation comparable to that represented in eq 15 occurs for $AgFAuF_6$, the $AgAuF_6$ product[14] is $Ag^IAu^VF_6$. The latter salt, like $Ag^IAsF_6$ and unlike $Ag^{II}Pt^{IV}F_6$, is oxidized by $O_2^+$ to give soluble Ag(II) species, and so the conversion to $Ag_3AuF_{12}$ is completed.

The $RuF_6^-$ species also has a favorable electron configuration (high-spin $dt_{2g}^3$) with favorable exchange energy. It is not a strong one-electron oxidizer[31] and, with $Ag^+$, gives $Ag^IRu^VF_6$. The oxidation of $AgFBF_4$ by $O_2RuF_6$ therefore is akin to the oxidations involving $O_2AsF_6$ and $O_2AuF_6$, and the product is clean $Ag_3RuF_{12}$.

Since, in strongly acidified aHF, where all Ag(II) is $Ag^{2+}$(solv), there is no oxidation by $O_2^+$ to give the $Ag_3MF_{12}$ salts and, on the other hand, basic or neutral aHF gives only $AgF_2$, it is clearly necessary to regulate closely the acidity of the aHF, if the $Ag_3MF_{12}$ salts are to be obtained efficiently in high purity. It appears that $BF_4^-$ provides the appropriate buffering control. This derives from the weak-acid nature of $BF_3$, which has low

(38) Lucier, G. M.; Shen, C.; Elder, S. H.; Bartlett, N. *Inorg. Chem.* **1998**, *37*, 3829−3834.

solubility in the aHF solvent. So, when $O_2MF_6$ acts as an oxidizer for $AgFBF_4$, it is the release of $BF_3$ that keeps the acidity essentially constant:

$$3AgFBF_4 + O_2MF_6 \rightarrow Ag_3MF_{12} + O_2(g) + 3BF_3(g) \quad (16)$$

As a consequence of the reactions expressed in eqs 8 and 9, the action of elemental fluorine on $AgFAsF_6$ converts one-third of the Ag(II) to Ag(III). The latter can be recovered as an alkali-metal $AgF_4^-$ salt by treating the black solid with alkali fluoride in aHF:

$$2F^-(solv) + (AgF)_2AgF_4AsF_6(c) \rightarrow 2AgF_2(c) + AgF_4^-(solv) + AsF_6^-(solv) \quad (17)$$

For the heavier alkali metals (K, Rb, Cs), the $AsF_6^-$ salts are of low solubility in aHF, whereas the $AgF_4^-$ salts are highly soluble. Therefore, this treatment provides for ready preparation of $AgF_4^-$ salts by room-temperature fluorination of $AgFAsF_6$ in aHF and without the need of photodissociation of the $F_2$. The latter is required[39] for the direct synthesis of $AgF_4^-$ from $AgF_2$ and $F_2$ in basic aHF.

It is surprising that the oxidation of Ag(II) in aHF (especially the interaction between $AgF_2$ and $O_2^+$ salts) should generate $(AgF)_2AgF_4MF_6$ and not the silver relative of $Au(AuF_4)_2Au(SbF_6)_2$. The mixed-valence gold compound[25] is the product of the action of fluorine on the salt $Au(SbF_6)_2$ in solution in aHF:

$$4Au^{2+}(solv) + 8SbF_6^-(solv) + F_2(g) \rightarrow Au(AuF_4)_2Au(SbF_6)_2(c) + 6SbF_5(solv) \quad (18)$$

The $[Au(AuF_4)_2Au]^{2+}$ component of the structure[25] is a slightly distorted relative of a puckered sheet of the $Ag^{II}F_2$ structure.[40,41] The $SbF_6^-$ species are packed closely between the $AuF_2$-composition sheets, as would be anticipated for the intercalation of $AuF_2$, if it existed and were isostructural with $AgF_2$. Yet the oxidation of $AgF_2$ has given (so far), not the related structure but, rather, $(AgF)_2AgF_4MF_6$. In passing, it should be noted that in $AgFRuF_6$ the Ag(II) coordination[31] is roughly square (and akin to that of Ag(II) in $AgF_2$),[40,41] so the failure to form the silver analogue of $Au(AuF_4)_2Au(MF_6)_2$ cannot be attributed to a distinct favoring of two-coordination by cationic Ag(II).

Comparison of the isostructural salts[42] $Ag^{2+}(SbF_6^-)_2$ and[25] $Au^{2+}(SbF_6^-)_2$ indicates that each $A^{2+}$ (A = Ag, Au) distorts the $SbF_6^-$ to the same extent, this despite the $Ag^{2+}$ having a higher first electron affinity[43] than $Au^{2+}$ (21.5 and 20.5 eV, respectively). It therefore remains possible that the $Ag(AgF_4)_2$-$Ag(SbF_6)_2$ relative of the gold compound may yet be made. A similar synthetic challenge is the preparation of a gold relative of the silver salts $(AuF)_2AuF_4MF_6$.

**Acknowledgment.** The authors gratefully acknowledge support from the National Science Foundation, under Grant No. DMR-9404755, and the Director, Office of Energy Research, Office of Basic Energy Sciences, Chemical Science and Materials Science Divisions of the U. S. Department of Energy, under Contract No. DE-AC-03-76SF00098. B.Ž. participated in the work during his tenure of a Miller Visiting Professorship (Spring Semester, 1993) for which professorship the Miller Institute, U.C. Berkeley, is thanked. O.G. also gratefully acknowledges the Alexander von Humboldt Foundation for a Feodor-Lynen Fellowship. Refinement of the $Ag_3AsF_{12}$ structure was completed with the assistance of Dr. F. Hollander of the U.C. Berkeley College of Chemistry CHEX-RAY facility.

**Supporting Information Available:** Listings of X-ray powder diffraction data, positional and thermal parameters, crystal data, and X-ray experimental details. This material is available via the Internet at http://pubs.acs.org.

IC9905603

(39) Lucier, G. M.; Whalen, J. M.; Bartlett, N. *J. Fluorine Chem.* **1998**, *89*, 101−104.
(40) Charpin, P.; Plurien, P.; Mereil, P. *Bull. Soc. Fr. Mineral. Cristallogr.* **1970**, *93*, 7.
(41) Jesih, A.; Lutar, K.; Žemva, B.; Bachmann, B.; Becker, S.; Müller, B. G.; Hoppe, R. *Z. Anorg. Allg. Chem.* **1990**, *588*, 77.
(42) Gantar, D.; Leban, I.; Frlec, B.; Holloway, J. H. *J. Chem. Soc., Dalton Trans.* **1987**, 2379.
(43) Moore, C. E. *Ionization Potentials and Ionization Limits Derived from the Analyses of Optical Spectra*; NSRDS-NBS 34; National Bureau of Standards: Washington, DC, 1970.